ELSEVIER

Microporous and Mesoporous Materials 27 (1999) 75–86

MICROPOROUS AND MESOPOROUS MATERIALS

On the synthesis of CoAPO-46, -11 and -44 molecular sieves from a $Co(Ac)_2 \cdot 4H_2O \cdot Al(iPrO)_3 \cdot H_3PO_4 \cdot Pr_2NH \cdot H_2O$ gel via experimental design

Qiuming Gao, Bert M. Weckhuysen *, Robert A. Schoonheydt

Centrum voor Oppervlaktechemie en Katalyse, Departement Interfasechemie, K.U. Leuven, Kardinaal Mercierlaan 92, 3001 Heverlee, Belgium

Received 25 May 1998; received in revised form 3 August 1998; accepted 14 August 1998

Abstract

The hydrothermal synthesis of cobalt-substituted microporous alumino-phosphates from an $r[Pr_2NH] \cdot [Co_xAl_{1-x}P_1]O_4 \cdot y[H_2O]$ gel is described. A well-defined set of experiments, based on an experimental design, was carried out in order to rationalize the influence of the crystallization time/temperature, and r, x and y of the initial gel on the isomorphous substitution of Co^{2+}. CoAPO-11, CoAPO-44, CoAPO-46 were the main crystalline materials obtained. These solids were characterized by X-ray diffraction (XRD), thermogravimetrical analysis (TGA), scanning electron microscopy (SEM), electron microscope microprobe analysis (EMMA) and diffuse reflectance spectra (DRS), which resulted in a quantitative model relating the synthesis conditions with the overall crystallinity. In addition, a relation between the overall crystallinity and the degree of isomorphous substitution has been established.

Keywords: Cobalt-substituted microporous alumino-phosphates; Crystallinity; Hydrothermal synthesis

1. Introduction

Transition-metal-ion-substituted microporous alumino-phosphates have attracted a great deal of attention in recent years, mainly because of their potential catalytic applications and the possible creation of new types of molecule-selective devices [1–3]. Isomorphous substitution, i.e. the replacement of P^{5+} and/or Al^{3+} by a tetrahedrally coordinated transition metal ion, has been reported in the literature for more than 17 elements [4]. However, only in the case of, e.g. Co^{2+}, has convincing spectroscopic evidence been provided to support the isomorphous substitution of Co^{2+} in the lattice [5–15]. The amount of truly isomorphously substituted Co^{2+} is, however, very limited, although very recently Stucky and co-workers have developed a novel synthesis route to increase the Co/Al ratio or substitution degree up to 90% [16].

There are a large number of variables, such as temperature and time, template type and content, water content, etc. which are known to influence the hydrothermal synthesis of molecular sieves. Most of these variables are not independent, and are influencing each other during the synthesis

* Corresponding author.
E-mail: bert.weckhuysen@agr.kuleuven.ac.be

1387-1811/99/$ – see front matter
PII: S1387-1811(98)00274-1

process. Moreover, it is almost impossible to study the influence of these variables on the hydrothermal synthesis in a reasonable timespan. One way to overcome this problem is by using experimental design [17,18]. This method allows a reduction in the number of experiments without losing significant information, and can be used to gain insight into the synthesis process.

In this work, an experimental design has been applied in order to rationalize the hydrothermal synthesis of cobalt-substituted microporous alumino-phosphates in terms of synthesis time and temperature, water content, template content and Co-content. The obtained solids were characterized by X-ray diffraction (XRD), thermogravimetrical analysis (TGA), scanning electron microscopy (SEM), electron microscope microprobe analysis (EMMA) and diffuse reflectance spectra (DRS). It will be shown that three distinct crystalline cobalt-substituted molecular sieves, namely CoAPO-11, -44 and -46, can be synthesized, starting from a $r[Pr_2NH]\cdot[Co_xAl_{1-x}P_1]O_4\cdot y[H_2O]$ gel. A quantitative model is proposed, which relates the variables with the overall crystallinity obtained, and allows us to propose optimal synthesis conditions for CoAPO-11, -44 and -46.

2. Experimental section

2.1. Synthesis procedure

The synthesis conditions and gel compositions were chosen according to an experimental design, which is outlined below. The general synthesis procedure was as follows. $Co(acetate)_2\cdot 4H_2O$ (Aldrich) was added to bidistilled water, under stirring, until complete dissolution. Aluminum triisopropoxide [$Al(iPrO)_3$] was then added under continuous stirring, followed by the dropwise addition of di-*n*-propylamine (Pr_2NH, Janssen Chimica, 99%). At last, H_3PO_4 (85 wt.% sol. in water, pro analyze, Janssen Chimica) was added to the mixture, and this final mixture was stirred for 30 min. To control the exothermicity of the reaction, all the reagents were cooled and mixed in an ice bath at 273 K. The obtained homogeneous gel was transferred to a 50 ml Teflon bottle, which was then inserted in a stainless-steel autoclave. The synthesis was performed statically at various temperatures, and the solids were recovered from the synthesis mixtures by centrifugation, followed by washing with bidistilled water, and dried at ambient temperature.

2.2. Characterization techniques

Powder XRD patterns of the as-synthesized samples were recorded on a Siemens D5000 diffractometer using CuKα radiation. The overall X-ray crystallinity of the solids was determined as the sum of the most intense peak of each individual crystalline phase obtained in the experimental design. The most intense peaks are at 2θ of 7.72°, 9.48°, 9.35°, 7.54° and 6.53° for CoAPO-46, CoAPO-44, CoAPO-11, A and B, respectively (vide infra).

TGA were performed on the powdered solids, typically 20–40 mg, using the TG-DTA92 of Setaram. All samples were measured in a dynamic atmosphere of dry helium. SEM was performed with a Phillips 515 microscope. The samples were suspended in acetone and treated ultrasonically for 15 min. A single droplet suspension was coated on an alumina support. The coated support was covered by a gold film after drying and vacuo treatment. EMMA was done on a JEOL superprobe 733 to evaluate the chemical composition of the solids. DRS in the UV-vis-NIR region were measured on a Varian Cary5 spectrophotometer at room temperature. The spectra were recorded against a halon white reflectance standard (Labsphere SRS-99-010) in the range 200–2500 nm. The computer processing of the spectra consisted of the following steps: subtraction of the baseline, conversion to wavenumbers, and calculation of the Kubelka–Munk (K–M) function. The spectra were deconvoluted into Gaussian bands using Grams/386 (Galacties Industries Inc.). The values of the K–M function were used for quantitative purposes.

3. Experimental design

In order to describe the hydrothermal synthesis of cobalt-substituted alumino-phosphates from an

$r[Pr_2NH]\cdot[Co_xAl_{1-x}P_1]O_4\cdot y[H_2O]$ gel, five variables or factors were selected to quantitatively describe the differences in crystallinity and the degree of isomorphous substitution of cobalt. The factors under study were: X_1, the synthesis time (days); X_2 or y, the amount of water (mole); X_3 or r, the amount of template (mole); X_4 or x, the amount of cobalt and X_5, the crystallization temperature (°C). Because the ([Co]+[Al])/[P] ratio was always one, the amount of Al and P could be directly calculated. The limits of each factor were as follows: X_1, 3–9 days; X_2, 50–150 mole; X_3, 1.8–2.2 mole; X_4, 0.05–0.15 mole and X_5, 160–200°C.

A 5-level central composite experimental design, generated by MODDE for Windows 3.0 (Umetri AB) resulted in a set of 29 experiments [19]. In this design, each factor can take three distinct values; i.e. a central value and two limits. The generated spreadsheet, containing information about the set of 29 experiments, i.e. experiment name, run order, experimental conditions for the different factors, the overall crystallinity of the obtained solids, the obtained phases and the degree of incorporation of Co^{2+}, are summarized in Table 1. Two of these experiments, i.e. N28 and N29, are replicates of the central point (N27), in order to study the reproducibility of the synthesis process.

4. Results and discussion

4.1. Hydrothermal synthesis

The set of 29 synthesis gels of Table 1 resulted in a series of blue, blue-pink and pink materials, which were first characterized by XRD. An overview of the different phases is compiled in Table 1. It is clear that three distinct single-phase and crystalline materials were obtained, namely: CoAPO-11 (sample N04), CoAPO-46 (sample N19) and CoAPO-44 (sample N24), together with some physical mixtures of two of these molecular sieves (e.g. sample N18). The corresponding powder XRD patterns of these single-phase and blue-colored materials are given in Fig. 1, and match well, both in intensity and 2θ values, with the patterns reported for $AlPO_4$-n structures, with $n=11$ (AEL), 44 (CHA) and 46 (AFS) in the literature [20,21]. No extra peaks or peak broadening were observed. SEM analysis confirmed the crystallinity and phase purity of these samples (Fig. 2). CoAPO-46, which has a two-dimensional structure with 12 rings, crystallizes as hexagonal prisms with sizes of 7–8 μm × 50 μm. The CoAPO-44 crystals have a cubic shape with a length of 6–7 μm, whereas CoAPO-11 forms agglomerates of hexagonals prisms. EMMA of these products gave the following chemical composition, which was close to the initial gel composition (Table 1):

$$CoAPO-11{:}(Co_{0.05}Al_{0.96}P_1)O_4$$

$$CoAPO-44{:}(Co_{0.14}Al_{0.86}P_1)O_4$$

$$CoAPO-46{:}(Co_{0.09}Al_{0.91}P_1)O_4$$

The formation of CoAPO-11 and CoAPO-46 from a $r[Pr_2NH]\cdot[Co_xAl_{1-x}P_1]O_4\cdot y[H_2O]$ gel is not totally unexpected because both MAPSO-46 (with M = Mg) and CoAPO-11 have been previously synthesized with di-*n*-propylamine as an organic template molecule [22–24]. However, di-*n*-propylamine is not known to act as a template in the synthesis of structure type 44, which is usually made in the presence of cyclohexylamine [24–26]. In addition, both AFS and CHA structure types are much less widely studied molecular sieves for the incorporation of transition metal ions, and to the best of our knowledge, no characterization studies of CoAPO-46 molecular sieves have been reported in the literature.

To investigate the thermal properties of the CoAPO-11, CoAPO-44 and CoAPO-46 molecular sieves, thermogravimetrical analysis was performed in a dynamic way by flowing a mixture of O_2 and He over the solids, and a typical result is given in Fig. 3 for CoAPO-46. The low temperature loss between 100–300°C is due to the desorption of water and the decomposition of dipropylamine occluded inside the channels. The high-temperature and sharp weight loss at around 400°C is attributed to the desorption and decomposition of protonated amines, balancing the framework negative charge. The exact temperature of this decomposition process is dependent on the molecular sieve type, i.e. at 400°C for CoAPO-46 and CoAPO-11 and at 460°C for CoAPO-44, and

Table 1
5-level circumscribed central composite experimental design generated by the MODDE program for the hydrothermal synthesis of CoAPO-*n* materials from an $r[Pr_2NH]\cdot[Co_xAl_{1-x}P_1]O_4\cdot y[H_2O]$ gel

Experiment number	Experiment name	Run order	Time (days)	y	r	x	Synthesis temperature (°C)	$[Co]_{tetra}$:$[Co]^a_{octa}$	XRD crystallinity[b]	Phase (CoAPO-*n* with $n=$)[c]
1	N01	27	3	50	1.8	0.05	200	13.63	754	11, 46, B
2	N02	18	9	50	1.8	0.05	160	0.3	0	Amorphous
3	N03	4	3	150	1.8	0.05	160	0.2	0	Amorphous
4	N04	26	9	150	1.8	0.05	200	13.16	1204	11
5	N05	3	3	50	2.2	0.05	160	0.1	0	Amorphous
6	N06	7	9	50	2.2	0.05	200	7.88	1023	B, 11
7	N07	10	3	150	2.2	0.05	200	7.67	755	11
8	N08	17	9	150	2.2	0.05	160	0.25	0	Amorphous
9	N09	15	3	50	1.8	0.15	160	0.5	0	Amorphous
10	N10	2	9	50	1.8	0.15	200	5.636	294	11, 46, Lazulite
11	N11	29	3	150	1.8	0.15	200	1.85	83	11, Lazulite
12	N12	25	9	150	1.8	0.15	160	0.25	0	Amorphous
13	N13	19	3	50	2.2	0.15	200	14.4	841	46, 44
14	N14	20	9	50	2.2	0.15	160	0.2	0	Amorphous
15	N15	16	3	150	2.2	0.15	160	0.2	0	Amorphous
16	N16	28	9	150	2.2	0.15	200	0.47	243	Lazulite
17	N17	22	3	100	2	0.10	180	0.2	0	Amorphous
18	N18	8	9	100	2	0.10	180	10.67	930	46, 44
19	N19	23	6	50	2	0.10	180	28	2162	46
20	N20	14	6	150	2	0.10	180	0.2	0	Amorphous
21	N21	12	6	100	1.8	0.10	180	6.25	217	46, A
22	N22	1	6	100	2.2	0.10	180	10.83	778	44, 46, A
23	N23	5	6	100	2	0.05	180	0.25	0	Amorphous
24	N24	6	6	100	2	0.15	180	8.78	960	44
25	N25	9	6	100	2	0.10	160	0.35	0	Amorphous
26	N26	24	6	100	2	0.10	200	13.23	1253	11, 46
27	N27	13	6	100	2	0.10	180	8.38	361	A
28	N28	21	6	100	2	0.10	180	8.37	352	A
29	N29	11	6	100	2	0.10	180	8.37	379	A

[a]This ratio was determined after deconvolution of the individual DRS spectra. The sum of the intensities of the triplet bands of tetrahedral Co was taken as a measure of $[Co]_{tetra}$, whereas the band intensity at 20 800 cm^{-1} was used for quantifying $[Co]_{oct}$.
[b]The overall crystallinity of the solids was determined as the sum of the most intense peak of each individual crystalline phase. The most intense peaks are at 2θ of 7.72°, 9.48°, 7.54° and 6.53° for CoAPO-46, CoAPO-44, CoAPO-11, A and B, respectively.
[c]The *d*-values for the unknown structures A and B, and for the dense phase Lazulite are as follows: A (13.5216; 12.0076; 9.3379; 6.7854; 4.3184; 3.5280; 2.8828; 2.6127; 2.2837; 1.8690); B (11.7162; 10.33; 8.152; 5.873; 5.180; 4.769; 4.083; 3.678; 3.535; 3.014; 2.987; 2.548; 2.108; 2.040; 1.966) and Lazulite (3.2078; 3.1075; 2.5340; 2.2388; 1.9931; 1.7963).

the amount of protonated amines equals the Co^{2+}-content of the molecular sieves.

Besides CoAPO-11, CoAPO-44 and CoAPO-46 (and mixtures of them), other phases are formed. Twelve out of 29 of the synthesis gels gave amorphous materials, which were always pink-colored. In addition, a dense phase Lazulite was formed. Finally, two phases, denoted as A and B, were synthesized, and their characteristic *d*-values are summarized in Table 1. It is not clear up to this point what the exact structure is of these two materials. However, because only phase A can be synthesized as a single phase with a relatively low crystallinity (Samples N27–N29), we will not further discuss these solids in detail.

4.2. Optimal conditions for the synthesis of CoAPO-11, CoAPO-44 and CoAPO-46 molecular sieves

One of the goals of this work was to explore the possibilities of an experimental design for deriving

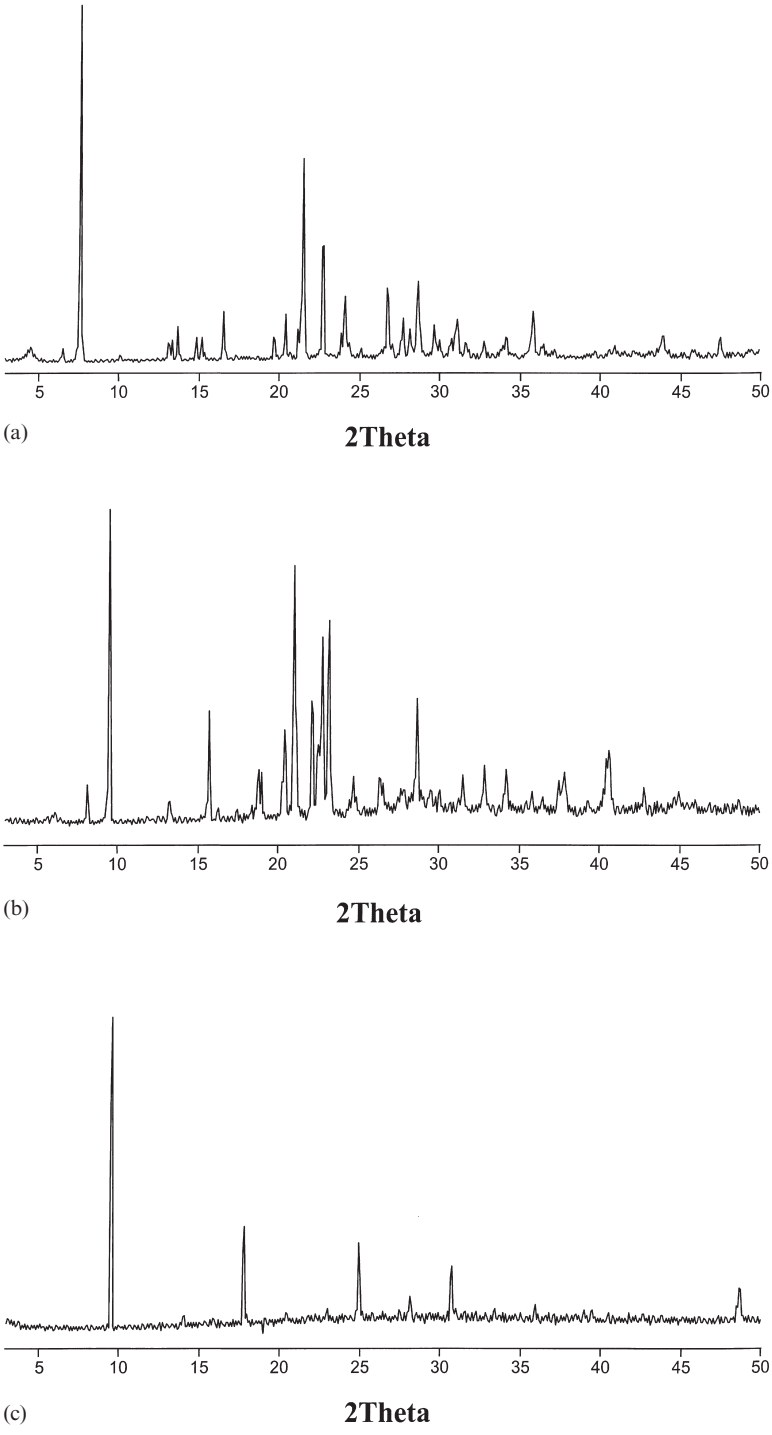

Fig. 1. X-ray diffraction patterns of as-synthesized CoAPO-46 (a), CoAPO-11 (b) and CoAPO-44 (c).

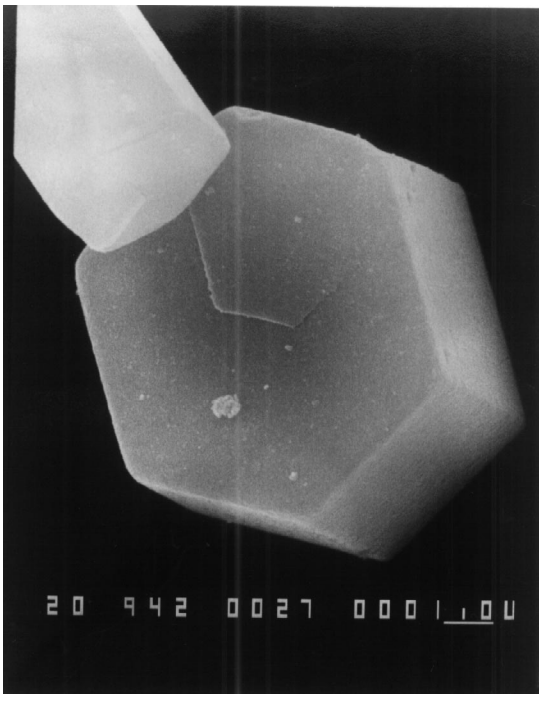

(a)

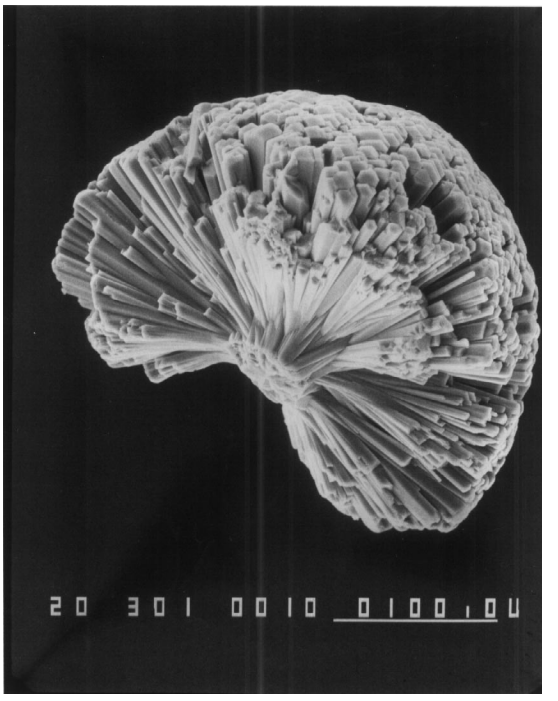

(b)

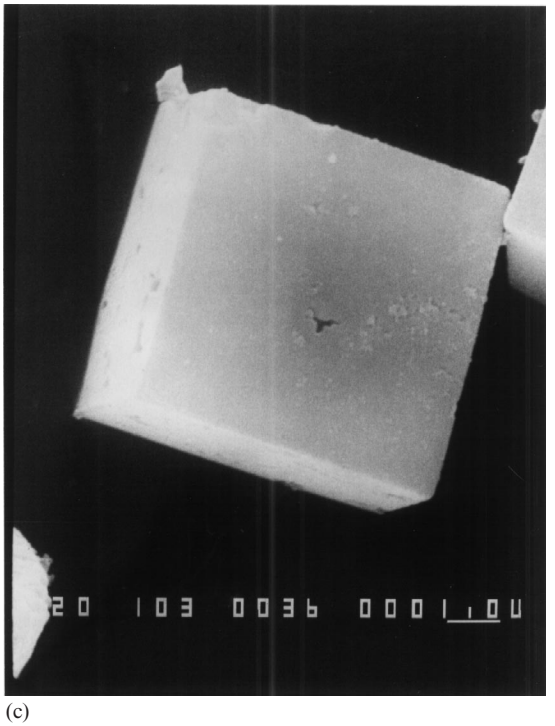

(c)

Fig. 2. Scanning electron micrograph of as-synthesized CoAPO-46 (a), CoAPO-11 (b) and CoAPO-44 (c).

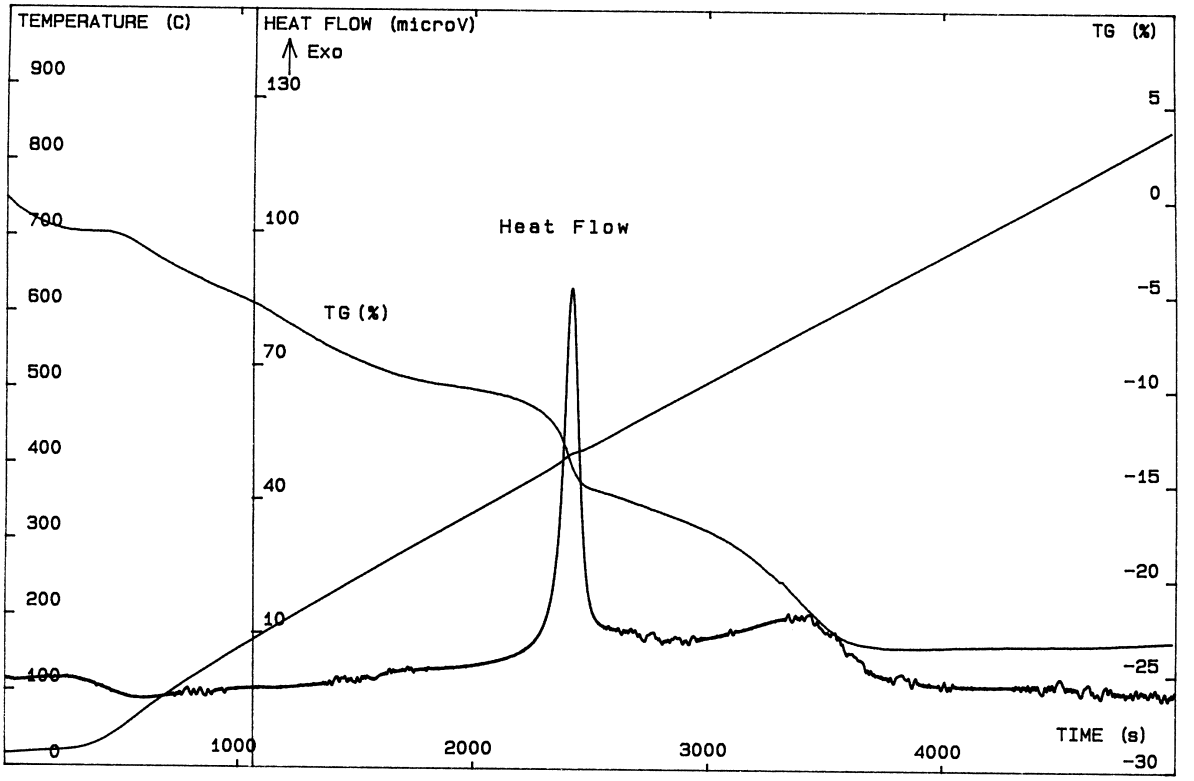

Fig. 3. Thermogravimetrical analysis of CoAPO-46.

the optimal conditions to synthesize highly crystalline single-phase molecular sieves out of a synthesis gel. The influence of the different design variables X_i (synthesis time and temperature; water content of the gel, y; template content of the gel, r; and Co content of the gel, x) and the response Y (XRD crystallinity) could be determined by applying a statistical model based on multiple linear regression (MLR). This analysis, which is extensively described in the literature [27], was done with the software package MODDE. The statistical model is based on the following equation:

$$Y=\beta_0+\sum_{i}^{5}\beta_i X_i+\sum_{i\neq j}\sum\beta_{ij}X_iX_j+\sum_{i}^{5}\beta_{ii}X_i^2 \qquad (1)$$

with Y the response; β_0 a constant; β_i the model coefficients for each factor; β_{ij} the model coefficients of the interaction terms; β_{ii}, the model coefficients of the quadratic terms; and X_i, the factor i. The 21 model coefficients β are calculated in order to minimize the sum of the residuals, which is defined as the quadratic difference between the observed and the predicted value of the response Y, i.e. the least-squares method.

First of all, we found that none of the calculated model coefficients β were appropriate for modelling the overall crystallinity of the solids with the different synthesis parameters. The complexity of the data of Table 1 resulted in model coefficients with too high p-values. The p-value is defined as the probability to obtain the value of the model coefficient if its own value is zero. A model coefficient β with a value of $p<0.05$ (95%) is called statistically significant, and must be included in the model. All other parameters may be excluded from the model.

In order to obtain more reasonable models, we have decided to model separately the synthesis of CoAPO-11, CoAPO-44 and CoAPO-46. Table 2 summarizes the eight model coefficients which can

Table 2
Optimized model coefficients β, together with the corresponding *p*-values, for the optimization of the synthesis of CoAPO-11

Model coefficient β	Scaled and centered value	*p*-value
β_1	−37.11	0.117
β_4	−77.667	0.00259
β_5	140.778	3.814×10^{-6}
β_{55}	140.778	0.001010
β_{14}	60.00	0.021
β_{15}	−41.750	0.098
β_{45}	−87.375	0.001588

be used to relate the synthesis time, synthesis temperature and the Co-content of the gel with the crystallinity of CoAPO-11. One can notice that all the parameters have appropriate *p*-values, with the exception of β_1 and β_{15}. In an analogous way, model coefficients can be obtained for optimizing the synthesis of CoAPO-44 and CoAPO-46 molecular sieves. The significance of the eight model coefficients of Table 2 can be evaluated by calculating the R^2 and Q^2 values (see Appendix A for definition). The R^2 value represents the percentage of the variation of the response explained by the statistical model, whereas Q^2 expresses the predictive power of the model. Both parameters are optimal if close to one. The model of Table 2 has R^2 and Q^2 values of 0.8101 and 0.5595, respectively, which indicates a statistically significant model with a medium predictive value. A final test to evaluate the statistical significance of the generated model can be done with the ANOVA (analysis of variance) method, which is outlined in Appendix B. The result of this analysis is the calculation of the *F*-value. The *F*-value for the model of Table 2 is 13, and represents a model which explains a significant fraction of the variance of the response. Summarizing, both the R^2/Q^2 and ANOVA analyses point towards a statistically meaningful mathematical model which relates, within the proposed limits of the experimental design, the XRD crystallinity of CoAPO-11 with the synthesis time, synthesis temperature and Co-content of the initial gel. Nevertheless, the medium predictive value of the model points towards the fact that some — still unknown — factors are not included in our analysis.

Table 2 also shows the presence of interaction terms, which describe the combined effect of two parameters on the crystallinity of the CoAPO-11 materials. The positive value of β_{14} indicates that both synthesis time and amount of cobalt are operating in the same direction, i.e. towards less crystalline materials, whereas the negative value of β_{15} points towards an opposite effect. The latter also holds for the interaction term β_{45}.

In order to visualize the significance of Eq. (1) and the model coefficients of Table 2, one can make crystallinity surface plots, as illustrated in Fig. 4. Fig. 4(a) predicts that the crystallinity of CoAPO-11 increases with increasing synthesis temperature and decreasing synthesis time, whereas Fig. 4(b) illustrates the combined effect of the Co-content and synthesis time on the crystallization process of CoAPO-11. The crystallinity of CoAPO-11 decreases with increasing Co-content and decreasing synthesis time. In other words, well crystalline single-phase CoAPO-11 materials can be best obtained from synthesis gels with low Co-content and which are autoclaved at 200°C for relatively short times. In this respect, it is important to mention the original recipe for $AlPO_4$-11 developed by Flanigen and co-workers [28]. These authors made their materials starting from a gel autoclaved at 200°C for 24 h.

In the case of CoAPO-46, the following optimal synthesis conditions were obtained: a synthesis temperature of 180°C, a gel with a relatively low water content and a synthesis time of about 6 days. The synthesis of CoAPO-44 requires also a temperature of 180°C, but synthesis time and water content seem to be less crucial. Because no synthesis conditions, in either the scientific or patent literature are reported for CoAPO-46 and CoAPO-44 (using an $r[Pr_2NH]\cdot[Co_xAl_{1-x}P_1]O_4\cdot y[H_2O]$ gel), it is not possible to compare our results with literature data. Summarizing, the optimal synthesis conditions for CoAPO-11, CoAPO-44 and CoAPO-46 molecular sieves from an $r[Pr_2NH]\cdot[Co_xAl_{1-x}P_1]O_4\cdot y[H_2O]$ gel can be obtained by applying an experimental design.

4.3. Spectroscopy

All the solids synthesized were characterized by DRS, and the DRS spectra of the highly crystalline

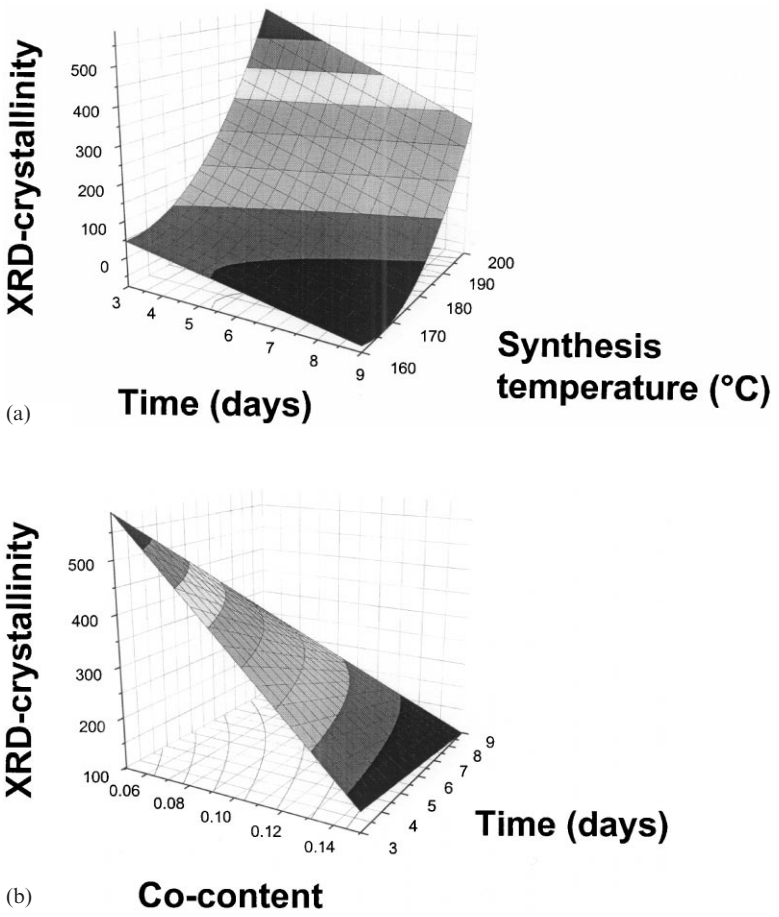

Fig. 4. (a) relation between the crystallinity of the solids and the synthesis temperature and time ([Co] = 0.05; CoAPO-11), and (b) relation between the crystallinity of the solids and the Co-content and synthesis time (synthesis temperature of 200°C and CoAPO-11).

single-phase CoAPO-11, CoAPO-44 and CoAPO-46 materials are shown in Fig. 5. The as-synthesized samples are characterized by a triplet in the visible region centered around 17 000 cm^{-1}, which is responsible for the blue color of the samples. Besides the triplet bands, a broad shoulder around 21 000 cm^{-1} is also apparent, and this shoulder is the most intense for the CoAPO-44 material. The triplet bands are usually assigned to tetrahedrally coordinated Co^{2+}, most probably located in framework positions, whereas the 21 000 cm^{-1} shoulder is typical for octahedrally coordinated Co^{2+} [29]. The latter assignment is confirmed by the presence of a 21 000 cm^{-1} band in the DRS spectra of the dense material Lazulite.

One can quantify the amount of octahedral and tetrahedral Co^{2+}-ions by deconvolution of the DRS spectra in a set of four bands, three of which belong to tetrahedral Co^{2+}, whereas the fourth band can be assigned to octahedral Co^{2+}. This is illustrated in Fig. 6 for sample no. 19 (CoAPO-46), sample no. 16 (Lazulite) and sample no. 11 (mixture of CoAPO-11 and Lazulite). In the case of CoAPO-46, a weak but clear shoulder centered around 20 800 cm^{-1} was revealed, whereas the triplet bands were centered at 16 000, 17 150 and 18 400 cm^{-1}. It is important to notice that only

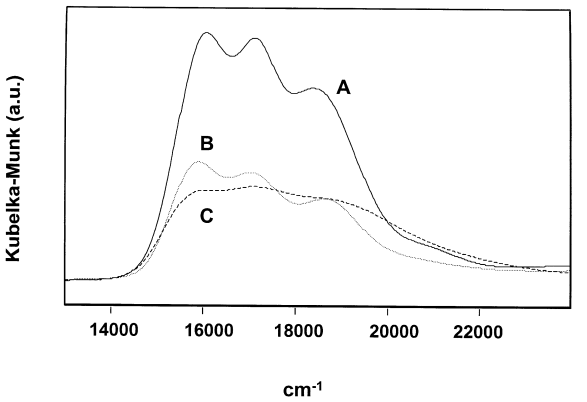

Fig. 5. Diffuse reflectance spectra of as-synthesized CoAPO-46 (a), CoAPO-11 (b) and CoAPO-44 (c).

minor changes in band positions were observed for the three crystalline materials, although in the case of CoAPO-44, the first two bands of the triplet are somewhat shifted to lower frequency. The dense phase Lazulite, which was pink-colored, was characterized by an intense band at 20 800 cm^{-1} [Fig. 6(b)], confirming the presence of octahedral Co^{2+}. However, it is also clear that small amounts of tetrahedral Co^{2+} were always visible. Mixed spectra were obtained for physical mixtures of the dense phase and a crystalline material, and for materials with low crystallinity. This is illustrated in Fig. 6(c) for a mixture of CoAPO-11 and Lazulite. In this case, a clear triplet and a broad band at 20 800 cm^{-1} were observed.

If one takes the sum of the intensities of the triplet bands as a measure of the amount of tetrahedral Co^{2+} ($[Co^{2+}]_{tetra}$), and the band intensity at 20 800 cm^{-1} as a quantitative measure for the amount of octahedral Co^{2+} ($[Co^{2+}]_{octa}$), one can determine the relative ratio $[Co^{2+}]_{tetra}$:$[Co^{2+}]_{octa}$ of each sample. These values, which can be regarded as a measure for the degree of isomorphous substitution, are compiled in Table 1. It is clear that well crystalline samples correspond with high $[Co^{2+}]_{tetra}$:$[Co^{2+}]_{octa}$. This is in line with the observation that high amounts of transition metal ions, such as Co and Cr, in the initial synthesis gel often have a negative influence on the overall crystallinity of the zeolite material [9,29,30]. The non-framework metal ions, which are preferably in octahedral coordination, can be

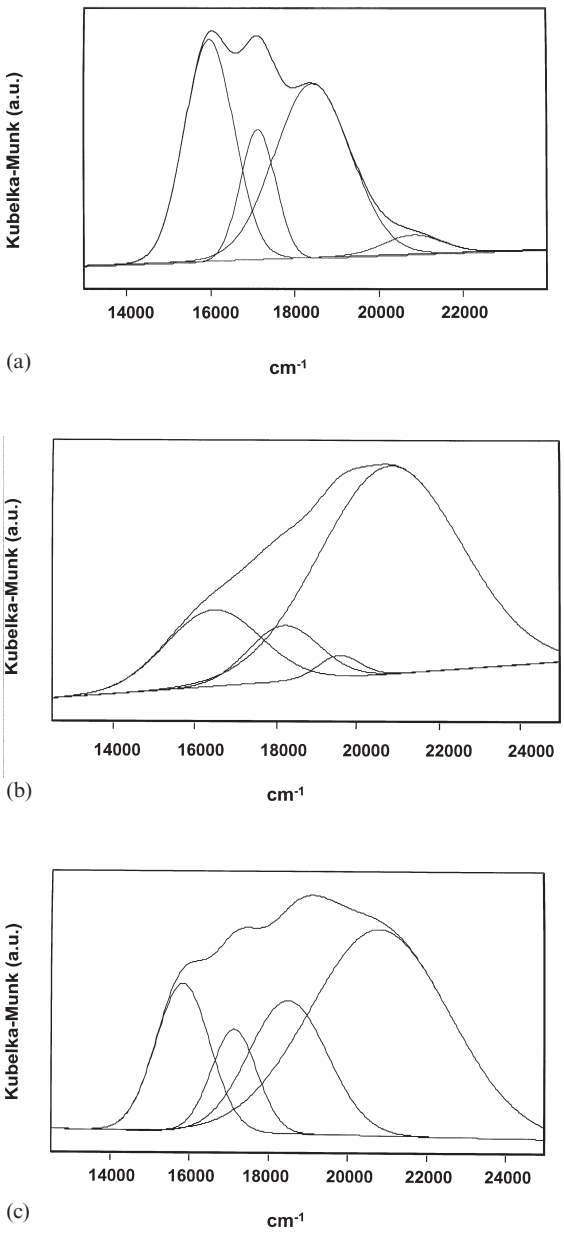

Fig. 6. (a) deconvolved diffuse reflectance spectrum of sample no. 19 (CoAPO-46), (b) deconvolved diffuse reflectance spectrum of sample no. 16 (Lazulite), and (c) deconvolved diffuse reflectance spectrum of sample no. 11 (mixture of CoAPO-11 and Lazulite).

washed off by centrifugation, or are present in the channels/cages or at the outer surface of the zeolites.

The obtained relation is given in Fig. 7, which

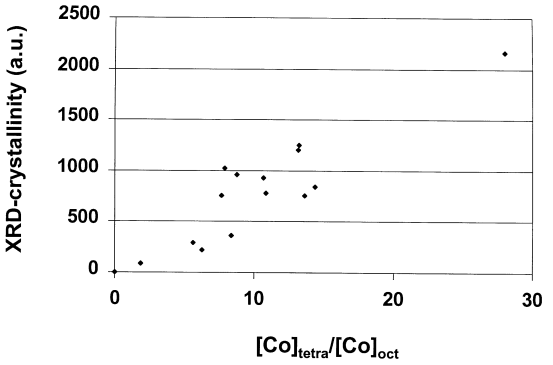

Fig. 7. Relation between the crystallinity, as determined by XRD, and the $[Co]_{tetrahedral}$:$[Co]_{octahedral}$ ratio of the solids, as revealed by deconvolution of the DRS spectra.

visually illustrates the relation between XRD-crystallinity and the $[Co^{2+}]_{tetra}$:$[Co^{2+}]_{octa}$ ratio of the solids. In this respect, the most crystalline material with the highest $[Co^{2+}]_{tetra}$:$[Co^{2+}]_{octa}$ ratio is CoAPO-46. Indeed, there were no extra inorganic phases in this sample, which could contain (octahedrally coordinated) cobalt.

5. Conclusions

The hydrothermal synthesis of CoAPO-11, -44 and -46 molecular sieves, and their physical mixtures have been achieved by using an experimental design with di-*n*-propylamine as the structure-directing agent. The optimal synthesis parameters for each of these solids have been determined, and the materials were characterized by various physicochemical methods, including TGA, DRS, SEM and EMMA. DRS confirms the partial formation of tetrahedrally coordinated cobalt, which is substituted into the alumino-phosphate framework.

Based on this work, the following conclusions can be made:

(1) Experimental design can be used to obtain optimal synthesis conditions for the hydrothermal synthesis of single-phase Co-containing molecular sieves.
(2) Water content and Co-content of the initial gel, together with synthesis time and temperature are important parameters, which allow the control of the final product of a hydrothermal synthesis process. The final structure type (AFS, AEL and CHA) of Co-containing molecular sieves can be controlled by choosing the appropriate synthesis conditions.
(3) The degree of isomorphous substitution of Co in the framework of microporous aluminophosphates seems to be related with the overall crystallinity of the solids.

Acknowledgements

This work was supported by the Fonds voor Wetenschappelijk Onderzoek (FWO) and the Geconcerteerde onderzoeksacties (GOA) of the Flemish Community. X.G. thanks the Research Council of K.U. Leuven for a junior postdoctoral fellowship, whereas B.M.W. acknowledges the FWO for a postdoctoral fellowship.

Appendix A

R^2 and Q^2test

R^2 and Q^2 are measures to evaluate the goodness of fit. R^2 is the percentage of the variation of the response explained by the model, whereas Q^2 is a measure for the predictive power of the model. They are defined as follows:

$$R^2 = SS_{regr}/SS_{total}$$

and

$$Q^2 = 1 - PRESS/SS_{total}$$

with:

$$SS_{total} = \sum_{i=1}^{n} (y_i - \bar{y})^2$$

$$SS_{regr} = \sum_{i=1}^{n} (\hat{y}_i - \bar{y})^2$$

$$SS_{res} = \sum_{i=1}^{n} (y_i - \hat{y}_i)^2$$

and

$$\mathrm{PRESS} = \sum_{i=1}^{n} \frac{(y_i - \hat{y}_i)^2}{(1-h_i)^2}$$

with h_i being the ith diagonal element of the matrix $\mathbf{X}(\mathbf{X}^{\mathrm{T}}\mathbf{X})^{-1}\mathbf{X}^{\mathrm{T}}$.

Appendix B

The analysis of variance (ANOVA) is a statistical technique to test the signifcance, particularly the lack of fit, of a mathematical model. The ANOVA analysis partitions the total variation of a selected response SS (sum of squares, corrected for the mean) into a part due to the regression model (SS_{regr}, sum of squares explained by the model) and a part due to the residuals (SS_{resid}, sum of squares not explained by the model), i.e. $SS = SS_{regr} + SS_{resid}$. For statistical reasons, one has to work with the mean sum of squares (MS), i.e. $MS_{regr} = SS_{regr}/Df_{regr}$ and $MS_{res} = SS_{res}/Df_{res}$ with D_f, the degree of freedom associated with the variance terms, and the square root of MS is the standard deviation, SD. The zero hypothesis H_0 is then that no model is necessary to describe the experimental results. The ratio MS_{regr}/MS_{res} is characterized by an F-distribution, and the ratio is defined as F. A small F resembles a model with no statistical meaning, whereas a large F is indicative for a statistically meaningful model.

References

[1] S.T. Wilson, E.M. Flanigen, in: M.L. Occelli, H.E. Robson (Eds.), Zeolite Synthesis, ACS Symposium Series, vol. 398, American Chemical Society, Washington, DC, 1989, p. 329.
[2] J.C. Vedrine, in: P.A. Jacobs, N.I. Jaeger, L. Kubelkova, B. Wichterlova (Eds.), Zeolite Chemistry and Catalysis, Studies in Surface Science and Catalysis, vol. 69, Elsevier, Amsterdam, 1991, p. 25.
[3] S.S. Lin, H.S. Weng, Appl. Catal. A 105 (1993) 289.
[4] S.T. Wilson, E.M. Flanigen, US patent no. 4 567 029, 1986.
[5] A.A. Verberckmoes, M.G. Uytterhoeven, R.A. Schoonheydt, Zeolites 19 (1997) 180.
[6] C. Montes, M.E. Davis, B. Murray, M. Narayana, J. Phys. Chem. 94 (1990) 6425.
[7] A.M. Prakash, M. Hartmann, L. Kevan, J. Phys. Chem. B 101 (1997) 6819.
[8] R.A. Schoonheydt, R. De Vos, J. Pelgrims, H. Leeman, in: P.A. Jacobs, R.A. Van Santen (Eds.), Zeolites: Facts, Figures, Future, Studies in Surface Science and Catalysis, vol. 49, Elsevier, Amsterdam, 1989, p. 559.
[9] M.G. Uytterhoeven, R.A. Schoonheydt, Microporous Mater. 3 (1994) 265.
[10] M.G. Uytterhoeven, W.A. Van Keyenberg, R.A. Schoonheydt, Mater. Res. Soc. Symp. Proc. 233 (1991) 57.
[11] M.P.J. Peeters, L.J.M. van de Ven, J.W. de Haan, J.H.C. van Hooff, Colloids Surfaces A: Physicochem. Engng Aspects 72 (1993) 87.
[12] V.P. Shiralkar, C.H. Saldarriaga, J.O. Perez, A. Clearfield, M. Chen, R.G. Anthony, J.A. Donohue, Zeolites 9 (1989) 474.
[13] G. Nardin, L. Randaccio, V. Kaucic, N. Rajic, Zeolites 11 (1991) 192.
[14] S.J. Hill, C.D. Williams, C.V.A. Duke, Zeolites 17 (1996) 291.
[15] L. Canesson, A. Tuel, Zeolites 18 (1997) 260.
[16] P. Feng, X. Bu, G.D. Stucky, Nature 388 (1997) 735.
[17] C.K. Bayne, I.B. Rubin, Practical Experimental Designs and Optimization Methods for Chemists, VCH, Deerfield Beach, FL, 1986.
[18] P. Box, W.G. Hunter, J.S. Hunter, Statistics for Experimenters, Wiley, New York, 1978.
[19] User's guide to Modde for Windows, Version 3.0 by Umetri AB, Statistical Modelling and Experimental Design, 1995, Umetri AB, Sweden.
[20] W.M. Meier, D.H. Olson, Ch. Baerlochter, Zeolites 17 (1996) 1.
[21] M.M.J. Treacy, J.B. Higgins, R. von Ballmoos, Zeolites 16 (1996) 323.
[22] C. Wee Lee, G. Brouet, X. Chen, L. Kevan, Zeolites 13 (1993) 565.
[23] N.N. Tusar, A. Tuel, I. Arcon, A. Kodre, V. Kaucic, in: H. Chon, S.-K. Ihm, Y.S. Uh (Eds.), Progress in Zeolite and Microporous Materials, Studies in Surface Science and Catalysis, vol. 105, Elsevier, Amsterdam, 1997, p. 501.
[24] J.M. Bennet, B.K. Marcus, in: P.J. Grobet, W.J. Mortier, E.F. Vansant, G. Schulz-Ekloff (Eds.), Innovation in Zeolite Materials Science, Studies in Surface Science and Catalysis, vol. 37, Elsevier, Amsterdam, 1989, p. 269.
[25] J. Batista, V. Kaucic, N. Rajic, D. Stojakovic, Zeolites 12 (1992) 925.
[26] U. Lohse, R. Bertram, K. Jancke, I. Kurzawski, B. Parlitz, E. Löffler, E. Schreier, J. Chem. Soc. Faraday Trans. 91 (1995) 1163.
[27] P. Box, N.R. Draper, Empirical Model-building and Response Surfaces, Wiley, New York, 1987.
[28] S.T. Wilson, S. Oak, B.M. Lok, E.M. Flanigen, US patent no. 4 310 440, 1982.
[29] A.A. Verberckmoes, B.M. Weckhuysen, R.A. Schoonheydt, Microporous Mesoporous Mater. 22 (1998) 165.
[30] B.M. Weckhuysen, R.A. Schoonheydt, Zeolites 14 (1994) 360.